Journal of Nano- and Electronic Physics
Vol. **14** No 1, 01001(6pp) (2022)

Журнал нано- та електронної фізики
Том **14** № 1, 01001(6cc) (2022)

Effect of Deuterium Ion Implantation Dose on Microstructure and Nanomechanical Properties of Silicon

A.S. Kuprin[1,*], S.N. Dub[2], A.S. Nikolenko[3], V.V. Strelchuk[3], O. Morozov[1], G.N. Tolmachova[1], A.O. Pudov[1]

[1] *National Science Center "Kharkov Institute of Physics and Technology", Kharkiv, Ukraine*
[2] *Bakul Institute for Superhard Materials, National Academy of Sciences of Ukraine, Kiev, Ukraine*
[3] *Institute of Semiconductor Physics, Kyiv, Ukraine*

(Received 12 April 2021; revised manuscript received 22 February 2022; published online 28 February 2022)

Implantation of hydrogen into silicon with subsequent annealing (Smart-Cut Technology) is applied to produce microelectronic devices. Improved characteristics of the resulting structures were achieved by using implantation of deuterium instead of hydrogen. The nanoindentation technique is widely used to measure the hardness H and elasticity modulus E of materials at the nanoscale. The aim of the present work is to investigate the influence of deuterium ion implantation dose on the structure and mechanical properties of single crystal silicon at the nanoscale. The influence of the deuterium ion implantation with an implantation dose ranging from 2×10^{15} to 1×10^{18} D/cm^2 on the structure and mechanical properties of single crystal silicon at the nanoscale has been investigated. Polished (111) silicon samples were implanted at 293 K by using a deuterium ion beam with an ion energy of 24 keV. It was shown by Raman spectroscopy that, depending on the implantation dose, three structural states are formed in silicon: a solid solution of deuterium (D) in Si, a solid solution mixed with the Si amorphous phase, and an amorphous state (a-Si:D) only. Thermal desorption (TD) spectroscopy shows that at low implantation doses, the deuterium TD spectra exhibit a single peak with a maximum at $T_{max} \sim 575$ K. At doses above 5×10^{17} D/cm^2, a low-temperature peak with a maximum at 500 K appears that is indicative of the formation of amorphous hydrogenated silicon a-Si:D. Nanoindentation tests have shown that in the regime of full plasticity in the indenter contact region (> 100 nm), the formation of deuterium solid solution in Si causes an increase in the sample surface hardness up to 14.1 GPa. The surface hardness sharply decreased down to 3.6 GPa with the a-Si:D layer formation.

Keywords: Silicon, Implantation, Deuterium, Raman spectroscopy, Thermal desorption, Nanoindentation.

DOI: 10.21272/jnep.14(1).01001

PACS numbers: 61.80.Jh, 61.82.Rx, 81.07.Bc, 61.05.cp, 61.46.Hk, 62.25. – g

1. INTRODUCTION

Silicon is the most common material in modern electronics. Implantation of hydrogen into silicon with subsequent annealing (Smart-Cut Technology) is applied to produce microelectronic devices. Improved characteristics of the resulting structures are achieved by using implantation of deuterium instead of hydrogen [1]. Nanomechanical properties of silicon have been studied rather well [2].

The nanoindentation technique is widely used to measure the hardness H and elasticity modulus E of materials at the nanoscale. During the tests, the indenter displacement h is continuously recorded as a function of the applied load P. After the tests, the unloading curve is analyzed [3]. The analysis provides data on the contact stiffness at peak load, and the hardness H and elasticity modulus E of the sample without measuring the indent sizes at depths that are much smaller than 1 μm.

The effects of implantation of different ions: Ar, C, N, Ne [4], C [5], Si [6] and Ti [7] on the mechanical properties of single crystal Si have been well studied, while the depth profile of Si hardness modified by the deuterium ion-beam implantation has not been studied sufficiently. In recent years, it has become popular to employ the nanoindentation technique in the continuous stiffness measurement (CSM) mode [8]. This mode enables one to determine the mean contact pressure P_{mean} as a function of the indenter displacement in the loading segment of the indentation curve. Analysis of the loading segment of the indentation curve provides knowledge of the hardness variation with depth in inhomogeneous materials.

However, the possibilities of nanoindentation in the CSM mode go beyond hardness measurements. A real Berkovich indenter is not ideally sharp and, as there is always some tip blunting, it is nearly spherical in shape. The tip radius of a new Berkovich indenter is equal to about 50 nm. This radius gradually increases as a result of hard materials testing and can reach from 300 to 400 nm after several years of service. Therefore, with penetration of the pyramidal Berkovich indenter into the sample surface, the plasticity nucleation in the contact region does not start at once, but only at a certain depth (generally, in the range of displacement h from 10 to 70 nm). In other words, the transition from elastic to elastoplastic deformation takes place in the contact area at the initial stage of the pyramidal indenter penetration. The elastoplastic transition during the indenter penetration makes it possible to measure the yield strength at the nanoscale even for hard brittle materials, nanocrystalline coatings, and c-BN single crystals. To our knowledge, there are only two publications dealing with the influence of irradiation on the onset of plasticity during nanoindentation [9, 10]. The

* kuprin@kipt.kharkov.ua

object of study was steel with a sharp elastoplastic transition ("pop-in"). It was demonstrated that the indenter load, which is necessary for the onset of plasticity in the contact area, decreased with an increase in the radiation dose.

The aim of the present work is to investigate the influence of deuterium ion implantation dose on the structure and mechanical properties of single crystal silicon at the nanoscale. To determine the mean contact pressure P_{mean} as a function of the indenter displacement and to find the parameters of the elastoplastic transition in the contact area, the nanoindentation technique in the CSM mode was used.

2. MATERIALS AND METHODS

Polished 500-μm thick (111) silicon plates were used in the experiments performed on the experimental facility "SKIF" [11]. The samples were exposed at room temperature (293 K) to deuterium ion beam with an energy of 12 keV/D (D_2^+ energy of 24 keV) at a current density of 5 μA/cm^2 and doses ranging from 2×10^{15} to 1×10^{18} D/cm^2.

Micro-Raman measurements were performed at room temperature in the backscattering configuration by using a triple Raman spectrometer T-64000 Horiba Jobin-Yvon, equipped with an electrically cooled CCD detector and an Olympus BX41 microscope. Lines of Ar-Kr ion lasers with wavelengths of 488 nm and 457 nm were used for excitation. The excitation light was focused onto the sample surface with a ×100/NA 0.9 optical objective giving a laser spot diameter of about 0.6 μm. A confocal pinhole of 100 μm was placed in the focal plane of the microscope to increase the spatial resolution.

Mechanical properties were studied by the nanoindentation technique on a Nanoindenter G200 device (KLA Corporation, USA). The tests were carried out in the CSM mode [8]. The load on the Berkovich indenter increased until the indenter displacement reached 200 nm. The tests were performed at a constant strain rate, which was equal to 0.05 s^{-1}. The CSM signal frequency was 45 Hz, the oscillation amplitude was 2 nm. Nanoindentation was performed with a Berkovich indenter with a tip radius of ~ 230 nm. On each sample, 10 indentations were made. To calibrate the shape function of the indenter, a standard fused silica sample was used.

3. RESULTS AND DISCUSSION

3.1. SRIM Modeling and Raman Spectroscopy

The profiles (Fig. 1) for the molecular deuterium D_2^+ ion beam implantation into silicon were calculated for an energy of 24 keV (12 keV per deuterium atom) using the Stopping and Range of Ions in Matter (SRIM) code [12]. As seen from the graph, at the highest implantation dose, the maximum of the deuterium atomic volume density profile exceeds even the volume density of silicon atoms (5×10^{22} cm^{-3}). Furthermore, the implantation of hydrogen into silicon is generally accompanied by the blistering effect, i.e., the formation of aggregates of hydrogen atoms, which afterwards results in defect production.

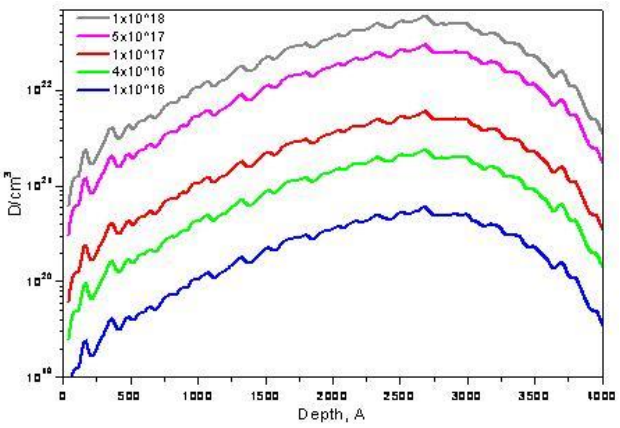

Fig. 1 – The depth profiles of the volume density of deuterium atoms in silicon. Each line corresponds to a different implantation dose in D/cm^2

Fig. 2 demonstrates that an increase in the implantation dose up to 4×10^{16} D/cm^2 leads to a gradual increase in the half-width of the phonon band of crystalline silicon c-Si (LO-TO). This corresponds to the deterioration of the silicon structural quality in the implantation region. At an implantation dose of 4×10^{16} D/cm^2 and higher, the spectra start to show wide phonon bands, denoted as a-Si (TA) and a-Si (TO), of the silicon amorphous phase. Higher implantation doses give rise to more pronounced phonon bands of the amorphous phase, which are accompanied by the intensity reduction of the c-Si (LO-TO) crystalline-phase band, which completely disappears in the spectrum for the highest implantation dose of 1×10^{18} D/cm^2.

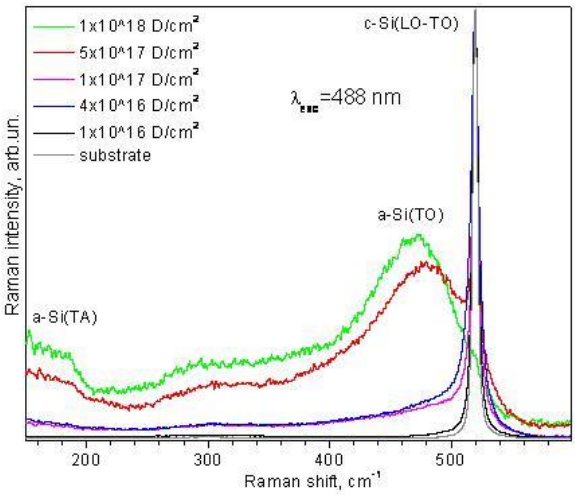

Fig. 2 – Raman spectroscopy of implanted Si at an excitation radiation wavelength of 488 nm

It should be noted that, with an excitation wavelength of 488 nm, due to strong absorption, the Raman signal in crystalline silicon is collected from a depth of ~ 520 nm. Thus, taking into account the depth of the maximum deuterium concentration from the implantation profile (Fig. 1), it is apparent that at low doses, the Raman spectrum shows a signal from both the implanted region and the substrate material underneath. With the amorphization of the implanted layer, the probing depth decreases, since the optical absorption

coefficient for amorphous silicon is almost an order of magnitude higher than that for crystalline silicon. Therefore, for the sample with the highest implantation dose, the signal from the substrate is no longer observed. In the high-frequency range (1300 to 1700 cm^{-1}), the spectra exhibit bands of local vibrations of hydrogen fixed on vacancy-type defects, denoted in Fig. 3 in accordance with the nomenclature of Ref. [13]. These bands are seen most clearly at the lowest irradiation dose and are gradually get washed out with increasing dose, probably due to the general amorphization and disordering of the silicon structure.

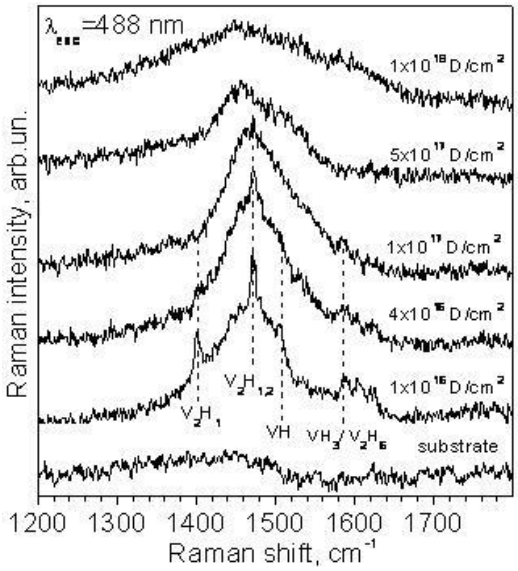

Fig. 3 – Raman spectra of implanted Si in the high-frequency range (1300 to 1700 cm^{-1}) measured at λ_{exc} = 488 nm

The probing depth decreases to about 310 nm upon switching to an excitation wavelength of 457 nm. As a whole, changes with increasing implantation dose in the 457-nm Raman spectra (Fig. 4) are similar to those in the 488-nm spectra.

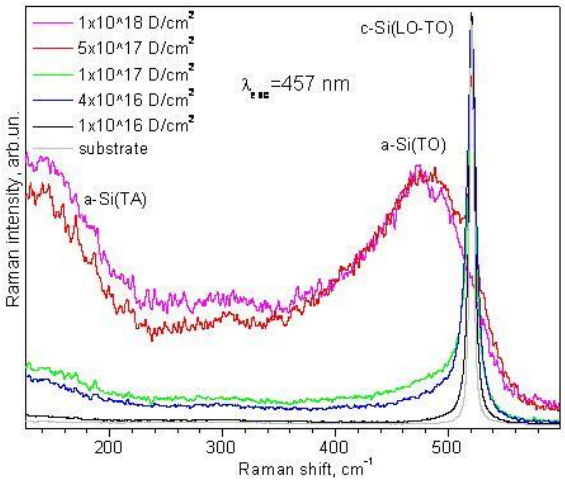

Fig. 4 – Raman spectra at λ_{exc} = 457 nm of Si samples implanted with different deuterium doses

Higher half-width values of the c-Si (LO-TO) phonon band at this excitation wavelength (Fig. 4) are due to a smaller influence on the signal of the substrate (underneath the implantation region), and hence, due to a greater contribution of the implantation region itself (with the worst crystal perfection) to the Raman spectrum.

For comparison, Fig. 5 shows the Raman spectra measured at two different excitation wavelengths for an implantation dose of 5×10^{17} D/cm^2.

It is evident that the relative intensity of the Raman signal from the c-Si substrate is lower at an excitation wavelength of 457 nm. This confirms our assumption that the registration of the c-Si (LO-TO) phonon band for a sample with this implantation dose is determined mainly by crystalline silicon, which is located below the implantation region.

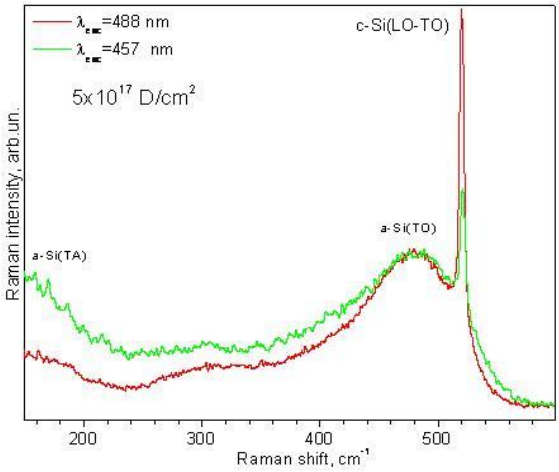

Fig. 5 – Raman spectra of Si implanted at a dose of 5×10^{17} D/cm^2 measured at two different excitation wavelengths (457 and 488 nm)

3.2. Thermal Desorption Spectroscopy

The representative spectra of deuterium Thermal Desorption (TD) for single crystal silicon samples implanted with deuterium ions at different doses are shown in Fig. 6. It can be seen that at low implantation doses, the deuterium TD spectra exhibit a single peak with a maximum at $T_{max} \sim 575$ K. The presence of the single peak points to the formation of deuterium solid solution in single crystal silicon. With increasing dose, the peak temperature remains practically unchanged. At the same time, the peak intensity increases and a moderate-intensity temperature-extended region of deuterium desorption starts to appear in the temperature range from 500 to 800 K. We identify this broadened temperature region of deuterium desorption as a result of implantation-induced amorphization of the silicon surface, since the Raman spectra in Fig. 2 show the formation of an amorphous phase in silicon at doses above 1×10^{17} D/cm^2.

At doses of 5×10^{17} D/cm^2 and above, a qualitative change in the deuterium TD spectrum takes place, which manifests itself in the appearance of a low-temperature region of deuterium desorption. The latter (a low-temperature peak with a maximum at 500 K) indicates the formation of amorphous hydrogenated silicon a-Si:D. The suggestion about the hydride formation is made based on our data from studies of the deuterium TD spectra measured for Pd and austenitic

stainless steel [14] samples. It was demonstrated there that the formation of hydrides manifests itself in the appearance of lower-temperature peaks in the deuterium TD spectra.

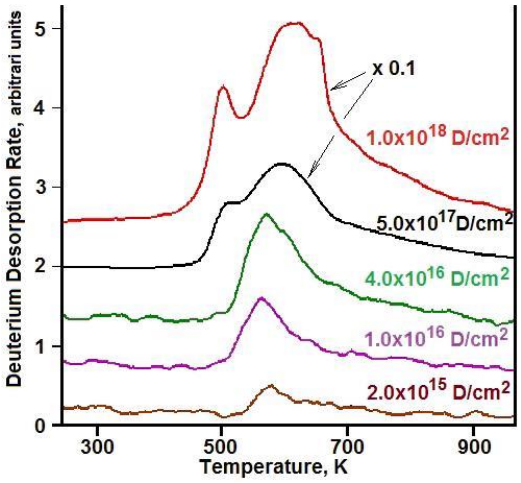

Fig. 6 – Deuterium TD spectra for silicon samples implanted with different deuterium doses

3.3. Nanoindentation

A typical load-displacement curve (P vs. h) of the Berkovich indenter penetration into silicon is shown in Fig. 7. The displacement of the indenter tip increases monotonically with the indentation load. Fig. 7 also illustrates the average contact pressure (ACP) dependence on the indenter displacement. Up to point A (h = 29 nm, P = 0.33 mN, ACP = 8.1 GPa), ACP increases directly proportional to the displacement (region I). Then, ACP continues to increase with the imprint depth, but not as fast as at the beginning (region II). After point B (h = 212 nm, P = 11.6 mN and ACP = 12 GPa), ACP does not change with the imprint depth (region III). When analyzing the ACP dependence on the displacement, one should keep in mind the pyramidal Berkovich indenter tip radius of about 230 nm. Thus, in the displacement range from 0 to 75 nm, the sample surface is deformed by a spherical tip. At displacements above 75 nm, the transition to a pyramidal indenter starts, but we were interested in the displacement range from 0 to 100 nm, where a spherical tip prevails in the contact area.

A similar ACP-displacement dependence was earlier observed by Tabor at the penetration of a spherical indenter into the surface of a previously plastically deformed sample of low-carbon steel [15]. The behavior of the ACP-displacement dependence observed by us is due to a change in deformation regimes in the contact area [15]. According to Tabor, in the first region, only elastic deformation took place in the contact area (see Fig. 7, region I). At point A, the critical shear stress under the contact reached the elastic limit of the sample, and a zone of contained plastic deformation is formed, which is surrounded by an elastically deformed material (Fig. 7, region II). With further load increase, the size of the zone of contained plastic deformation grows, and at point B it breaks out on the sample surface. At this moment, the regime of full plasticity in the contact area (Fig. 7, region III) begins. Thus, at point A, the nucleation of plasticity in the contact area takes place, and AB region is the elastoplastic transition in the contact area. The hardness measurements become possible only after the onset of the full plasticity regime in the contact area.

As it was noted above, at a displacement of less than 75 nm, the tests were performed by the spherical tip of the Berkovich pyramidal indenter. Therefore, for the analysis of the initial region of the loading curve before the onset of the elastoplastic transition, we used Hertz analysis. For a spherical indenter, the maximum contact pressure P_{max} and the average contact pressure P_{mean} (Meyer hardness) are defined as [15]:

$$P_{\max} = \left(\frac{6PE_r^2}{\pi^3 R^2}\right)^{1/3}, \; P_{mean} = \frac{2}{3}P_{\max}, \tag{1}$$

where E_r is the reduced elastic modulus, P is the load, R is the radius of the spherical indenter. The maximum shear stress is equal to [15]:

$$\tau_{\max} = \frac{1}{2}|\sigma_1 - \sigma_3|, \tag{2}$$

where σ_1 and σ_3 are the principal stresses.

The τ_{max} reaches a maximum value (τ_c) directly under the center of the contact area (r = 0) at a distance of 0.48×a under the sample surface, where a is the contact radius [16]:

$$\tau_c = [0.61 - 0.23(1 + \nu)]P_{max} \approx 0.31P_{max} \approx 0.47P_{mean}, \tag{3}$$

where ν is the Poisson's ratio.

The effect of deuterium implantation dose on the mechanical properties (hardness H, Young's modulus E, plasticity nucleation P_c, shear stress τ_c) of single crystal silicon is presented in Table 1.

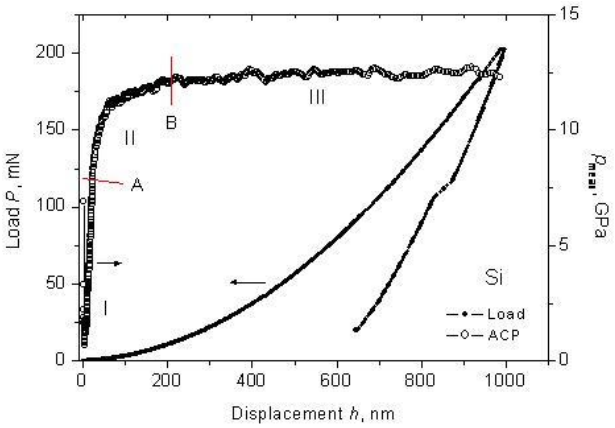

Fig. 7 – The load-displacement curve and the dependence of ACP on the indenter displacement for an untreated (111) silicon: point A is the onset of plasticity in the contact area, region AB is a smooth elastic-plastic transition. Deformation regimes in the contact area: region I is the elastic region, region II is the contained plasticity regime, region III is the full plasticity regime in the contact area

Hence, the calculated yield strength of single crystal silicon at the nanoscale was 8.8 GPa. Generally, after electropolishing, chemical etching, annealing, the sur-

face layer of crystalline samples with a low dislocation density shows an abrupt elastoplastic transition ("pop-in"), which results from homogeneous dislocation nucleation at shear stresses close to the theoretical shear strength. A smooth elastoplastic transition was previously observed only for materials with a high dislocation density, either in the bulk (e.g., plastically pre-strained metals and nanocrystalline materials [17]) or in the surface layer of the sample (after mechanical polishing of the surface [17].

Table 1 – The effect of deuterium implantation dose on the mechanical properties of single crystal silicon

Dose, D/cm^2	Structure	E, GPa	H, GPa	P_c, GPa	τ_c, GPa
–	Initial	187 ± 3	11.8 ± 0.3	7.8 ± 0.7	3.6 ± 0.3
2×10^{15}	solid solution	169 ± 2	13.6 ± 0.2	8.6 ± 0.7	4.0 ± 0.3
1×10^{16}	solid solution	184 ± 2	14.0 ± 0.2	8.3 ± 0.6	3.9 ± 0.3
4×10^{16}	solid solution	177 ± 3	14.2 ± 0.4		
6×10^{16}	amorphous, solid solution	173 ± 3	13.7 ± 0.4	7.9 ± 0.5	3.7 ± 0.2
1×10^{17}	amorphous, solid solution	163 ± 3	14.1 ± 0.3	8.0 ± 0.6	3.7 ± 0.3
5×10^{17}	a-Si:D	126 ± 2	6.8 ± 0.2	2.9 ± 0.4	1.4 ± 0.2
1×10^{18}	a-Si:D	84 ± 2	3.6 ± 0.1	3.7 ± 0.5	1.7 ± 0.2

For these materials, the plasticity nucleation with indenter penetration is associated with the motion and multiplication of dislocations that already exist in the contact region. So, for the initial (unimplanted) single crystal silicon, we observe anomalous mechanics, i.e., the indentation curve shows no "pop-in" phenomena. This was also noted elsewhere [17]. It is likely that the anomalous mechanical behavior of single crystal silicon is due to the fact that, during the indenter penetration into silicon, a pressure-induced phase transformation takes place in the imprints (the atoms are more densely packed, i.e., a first-order phase transition occurs). At a pressure of about 12 GPa, common brittle silicon Si-I having a diamond lattice is transformed into a plastic high-pressure metallic phase Si-II having a β-tin lattice. And only after that, plastic flow in the contact area starts. In other words, the mechanism of silicon plastic deformation is caused by the high pressure of the phase transition in the contact region. Here, there is some discrepancy considering that the pressure of Si-II generation is equal to 12 GPa, while in our case, plasticity in the contact region nucleated at 8 GPa. It can be suggested that the pressure value of 12 GPa is for the case of hydrostatic compression. But under the contact area, not only high pressure arises, but also high shear stresses. It is well known that shear stresses reduce the phase transformation pressure [17].

The formation of a solid solution of deuterium in single crystal silicon with exposure to deuterium ions at a dose of 2×10^{15} D/cm^2 causes an increase in hardness from 11.8 up to 13.6 GPa. In the dose range from 2×10^{15} to 4×10^{16} D/cm^2, the silicon near-surface layer (h = 100 to 200 nm) hardness increases up to 14.2 GPa (Fig. 8, Table 1). The onset of the solid solution and amorphization (1×10^{17} D/cm^2) has no effect on the gradual decrease in the elastic modulus, and only after the a-Si:D layer formation on the sample surface, it leads to a sharp reduction in hardness, elastic modulus and yield point (Fig. 8). The sample implanted with the highest dose of 1×10^{18} D/cm^2 shows the sharp yield point formation at a depth of about 20 nm, although at a depth of ~ 50 nm, the hardness of the sample is significantly lower than that of the sample implanted with 5×10^{17} D/cm^2. Hardness (3.6 GPa) and Young's modulus (84 GPa) obtained for a sample with a-Si:D layer (dose 1×10^{18} D/cm^2) showed a quite good correlation with the mechanical properties (H = 3.8-4.9 GPa and E = 25-45 GPa) of hydrogenated nanocrystalline silicon thin films [18].

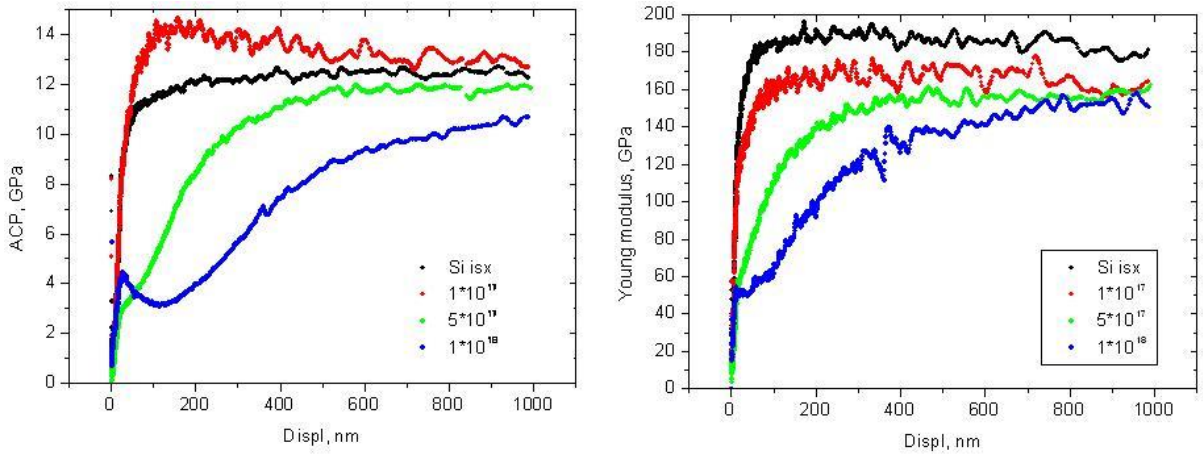

a b

Fig. 8 – Average contact pressure (a) and Young's modulus (b) versus the indenter displacement into the silicon surface

4. CONCLUSIONS

In the present work, the influence of deuterium ion implantation with implantation doses ranging from 2×10^{15} to 1×10^{18} D/cm^2 at the nanoscale level on the structural and mechanical properties of single crystal silicon has been investigated.

It is shown by Raman spectroscopy that in the range of implantation doses from 2×10^{15} to 4×10^{16} D/cm^2, deuterium in silicon is in solid solution. For doses from 6×10^{16} to 1×10^{17} D/cm^2, a mixture of a solid solution and an amorphous silicon phase is formed. For doses $\geq 10^{17}$ D/cm^2, only an amorphous state in silicon is formed.

TD spectroscopy shows that at low implantation doses, the deuterium TD spectra exhibit a single peak with a maximum at $T_{max} \sim 575$ K. At doses above 5×10^{17} D/cm^2, a low-temperature peak with a maximum at 500 K appears, that is indicative of the formation of amorphous hydrogenated silicon a-Si:D.

A sharp ACP increase in the initial phase (h up to 100 nm for the untreated Si sample) displays the elastoplastic transition in the contact area. In the full plasticity regime in the contact area (h > 00 nm), the formation of deuterium solid solution in silicon causes an increase in the sample surface hardness up to 14.1 GPa. The surface hardness sharply decreases to 3.6 GPa with the a-Si:D layer formation.

REFERENCES

1. D. Misra, R.K. Jarwal, *Appl. Phys. Lett.* **76**, 3076 (2000).
2. G.M. Pharr, *Mater. Res. Soc. Symp. Proc.* **239**, 301 (1992).
3. W.C. Oliver and G.M. Pharr, *J. Mater. Res.* **7**, 1564 (1992).
4. Zhi-Hui Xu, Young-Bae Park, Xiaodong Li, *Mater. Res.* **25**, 880 (2010).
5. P. Mishra, S.R. Bhattacharyya, D. Ghose, *Nucl. Instr. Methods Phys. Res. B* **266**, 1629 (2008).
6. D.M. Follstaedt, J.A. Knapp, S.M. Myers, *J. Mater. Res.* **19**, 338 (2004).
7. B. Nunes, P. Nolascoa, A.P. Serroa, E. Alves, R. Colaço, *Nucl. Instr. Methods Phys. Res. B* **471**, 69 (2020).
8. J. Hay, P. Agee, E. Herbert, *Exp. Tech.* **3**, 86 (2010).
9. Siwei Chen, Yongming Wang, Naoyuki Hashimoto Somei Ohnuki, *Phil. Mag. Lett.* **94,** 433 (2014).
10. K. Jin, Y. Xia, M. Crespillo, H. Xue, Y. Zhang, Y.F. Gao, H. Bei, *Scripta Mater.* **157**, 49 (2018).
11. V.V. Ruzhitsky, Yu.A. Gribanov, V.F. Rybalko, S.M. Khazan, A.N. Morozov, I.S. Martynov, *Probl. Atom. Sci. Technol.,* **51** 84 (1989) [in Russian].
12. http://www.srim.org.Version-SRIM-2006.02.
13. O. Moutanabbir, B. Terreault, M. Chicoine, F. Schiettekatte, P.J. Simpson, *Phys. Rev. B* **75**, 075201 (2007).
14. O. Morozov, V. Zhurba, I. Neklyudov, O. Mats, V. Progolaieva, V. Boshko, *Nanoscale Res. Lett.* **11**, 44 (2016).
15. D. Tabor, *Hardness of metals* (Oxford: Clarendon Press: 1951).
16. K.L. Johnson, *Contact Mechanics* (Cambridge University Press: 1985).
17. O.G. Lysenko, S.N. Dub, V.I. Grushko, E.I. Mitskevich, G.N. Tolmacheva, *J. Superhard Mater.* **35**, 350 (2013).
18. L. Guo, J. Ding, J. Yang, G. Cheng, Z. Ling, *Surf. Interface Anal.* **44**, 265 (2012).

Вплив дози імплантованих іонів дейтерію на мікроструктуру і наномеханічні властивості кремнію

О.С. Купрін[1], С.М. Дуб[2], А.С. Ніколенко[3], В.В. Стрельчук[3], О. Морозов[2], Г.М. Толмачова[1], О.О. Пудов[1]

[1] *Національний науковий центр Харківський фізико-технічний інститут, Харків, Україна*
[2] *Інститут надтвердих матеріалів імені В.М. Бакуля НАН України, Київ, Україна*
[3] *Інститут фізики напівпровідників, Київ, Україна*

Імплантація водню в кремній з подальшим відпалом (технологія Smart-Cut) застосовується для виготовлення мікроелектронних пристроїв. Покращені характеристики отриманих структур були досягнуті шляхом імплантації дейтерію замість водню. Метод наноіндентування широко використовується при вимірюванні твердості H та модуля пружності E матеріалів у нанорозмірному масштабі. Метою даної роботи є дослідження впливу дози імплантації іонів дейтерію на структуру та механічні властивості монокристалічного кремнію в нанорозмірному масштабі. Досліджено вплив доз імплантації іонів дейтерію в діапазоні від 2×10^{15} до 1×10^{18} D/см^2 на структуру та механічні властивості монокристалу кремнію в наномасштабі. Зразки полірованого кремнію (111) імплантували при 293 К пучком іонів дейтерію з енергією 24 кеВ. Методом Раманівської спектроскопії було показано, що в залежності від дози імплантації в кремнії утворюються три структурні стани: дейтерій знаходиться у твердому розчині, суміш аморфної фази кремнію і твердого розчину, і тільки аморфний стан (a-Si:D). Термічна десорбційна спектроскопія показує, що при низьких дозах імплантації в спектрах термодесорбції дейтерію спостерігається один пік з максимумом при $T_{max} \sim 575$ К, а при дозах вище 5×10^{17} D/см^2 з'являється низькотемпературний пік з максимумом при 500 К, що свідчить про утворення аморфного гідрогенізованого кремнію a-Si:D. Наноіндентування показало, що в режимі повної пластичності в контакті (> 100 нм), утворення твердого розчину дейтерію в кремнії спричиняє збільшення твердості поверхні зразка до 14,1 ГПа. Твердість поверхні різко зменшується до 3,6 ГПа з утворенням шару a-Si:D.

Ключові слова: Кремній, Імплантація, Дейтерій, Раманівська спектроскопія, Термічна десорбція, Наноіндентування.